Electronic Supplementary Information accompanying the paper:

Coordinated nitrate anions can be directional π-hole donors in the solid state; a CSD study

Tiddo J. Mooibroek

van 't Hoff Institute for Molecular Sciences, Universiteit van Amsterdam, Science Park 904, 1098 XH Amsterdam, The Netherlands; E-mail: t.j.mooibroek@uva.nl

Details of methodology and overview of supporting material 2

Table S1 Numerical overview of CSD searches performed 7
Table S2 Overview of close contacts with sp^2 O-atoms 16

Figure S1 Possible coordination modes found for an NO_3^- anion 3
Figure S2 Distribution of metals coordinated by a nitrate anion in any fashion 4
Figure S3 Distribution of metals η^1 coordinated by a nitrate anion 5
Figure S4 Distribution of metals η^2 coordinated by a nitrate anion 6
Figure S5 Simplified schematic of the most general query used 8
Figure S6 3D, 4D and *N*(***r***) plots for any coordination mode and any **ElR** 8
Figure S7 3D, 4D and *N*(***r***) plots for any coordination mode and any **N** 8
Figure S8 3D, 4D and *N*(***r***) plots for any coordination mode and any **O** 9
Figure S9 3D, 4D and *N*(***r***) plots for any coordination mode and any **S** 9
Figure S10 3D, 4D and *N*(***r***) plots for any coordination mode and any **Cl** 9
Figure S11 3D plots for any coordination mode and any **F**, **P**, **As**, **Se**, **Br** or **I** 10
Figure S12 3D, 4D and *N*(***r***) plots for any coordination mode and **R=O** 10
Figure S13 3D, 4D and *N*(***r***) plots for any coordination mode and **ROH** 11
Figure S14 3D, 4D and *N*(***r***) plots for any coordination mode and **H_2O** 11
Figure S15 3D, 4D and *N*(***r***) plots for η^1 NO_3^- with **ElR**, **ROH** and **R=O** 12
Figure S16 3D, 4D and *N*(***r***) plots for η^2 NO_3^- with **ElR**, **ROH** and **R=O** 13
Figure S17 3D, 4D and *N*(***r***) plots for $2\eta^1\mu$ and $2\eta^1\mu$ NO_3^- with **ElR**, **ROH** and **R=O** 14
Figure S18 3D plots for $\eta^2\eta^1$, $2\eta^2\mu$ and $3\eta^1\mu$ NO_3^- with **ElR**, **ROH** and **R=O** 15

References ……
19

Details of methodology and overview of supporting material

The CSD[1] version 5.37 (November 2015, including three updates (until May 2016)) was inspected on the 23rd of march 2017 using ConQuest (version 1.19) and the data was limited to high quality structures (R ≤ 0.1), excluding structures determined by powder diffraction. An initial dataset was created that contained a NO_3^- anion with at least one of its O-atoms attached to a metal (NB: the PDB was also inspected with an identical query using Relibase, but no such structures could be retrieved). This query yielded 11,208 crystallographic information files (CIFs). This dataset was further dissected by using as discriminators the number of metals attached to NO_3^-, the coordination mode in terms of hapticity (η) and the possible bridging function of an O-atom (μ). The type of metal atom and its charge were left unspecified. This resulted in the 27 different datasets as specified in Figure S1.

To obtain some idea about what metals are most frequently coordinated by nitrate anions, three separate searches were performed: one for the largest (initial) dataset containing any type of nitrate coordination; one limited to η^1 coordinated NO_3^- and one limited to η^2 coordinated NO_3^-. These data were analyzed and the relative occurrence for each metal was projected on a periodic table as shown in Figures S2 – S4.

Shown in Table S1 is a numerical overview of the data that was obtained to assess possible π-hole interactions with coordinated nitrate. Figure S5 represents a simplified schematic for the most general query used to generate these data. For this most generic search, a dataset was created that contained a NO_3^- anion with at least one of its O-atoms attached to a metal (M) and an intermolecular N···electron rich atom (ElR) distance (***d***) of ≤ 5 Å (ElR = N, P, As, O, S, Se, Te, F, Cl, Br, I or At). All data are thus confined to a sphere with 5 Å radius, centered on NO_3^-. Due to symmetry and for ease of interpretation the data are displayed within a hemisphere. Cartesian coordinates of ElR and the central nitrate were derived as described elsewhere.[2] These coordinates were plotted in a three dimensional plot. Four dimensional density plots were also generated, using 405 grids (X [$9\times{}^{10}/_{9}$ Å], Y [$9\times{}^{10}/_{9}$ Å], Z [5×1 Å]).[3] To assess possible van der Waals overlap between ElR and the N-atom of the coordinated nitrate anion, the parallel displacement parameter (***r***, see also Figure S5) for ElR was derived[4] and the data characterized by $\boldsymbol{r} \leq 1$ Å was plotted as a function of the van der Waals corrected N···ElR distance in an $N(\boldsymbol{r})$ plot. These plots (3D/4D/$N(\boldsymbol{r})$) for this most general query (any ElR, 82,338 hits in 9,288 CIFs) are collected in Figure S6.

This dataset is likely too diverse and was thus scrutinized further based on the binding motif (as illustrated in Figure S1) and the identity of ElR. A numerical overview of all the data is given in Table S1 and relevant plots were only generated in case of sufficient data. First, the data found for any ElR was split up into individual ElR atoms (N, O, F, etc.). Relevant plots for this data are given in Figures S7 – S11. As ElR = O appeared most abundant (45,859 hits in 7,971 CIFs), these data were further split into sp^2 (R=O) and sp^3 hybridized oxygen (ROH and H_2O). To exclude coordinated and protonated O's, these searches were repeated specifying that the O-atom should only be bound as prescribed by its hybridization (i.e. one atom attached for sp^2 and two atoms attached for sp^3 hybridization). Relevant plots for these comparative datasets are given in Figure S12 (R=O), Figure S13 (ROH) and Figure S14 (H_2O) As these comparative plots appeared rather similar, the data presented in the main text has been limited to selected uncoordinated/unprotonated O-derivatives interacting with a coordinated nitrate anion. Next, the binding motifs that were identified in at least 50 CIFs were analyzed considering any electron rich atom (ElR) and uncoordinated/unprotonated sp^2 (R=O) and sp^3 OH's (ROH). This gave three datasets for each nitrate binding motif considered, as detailed in Table S1. All relevant plots for these seven data are shown in Figures S15 – S18.

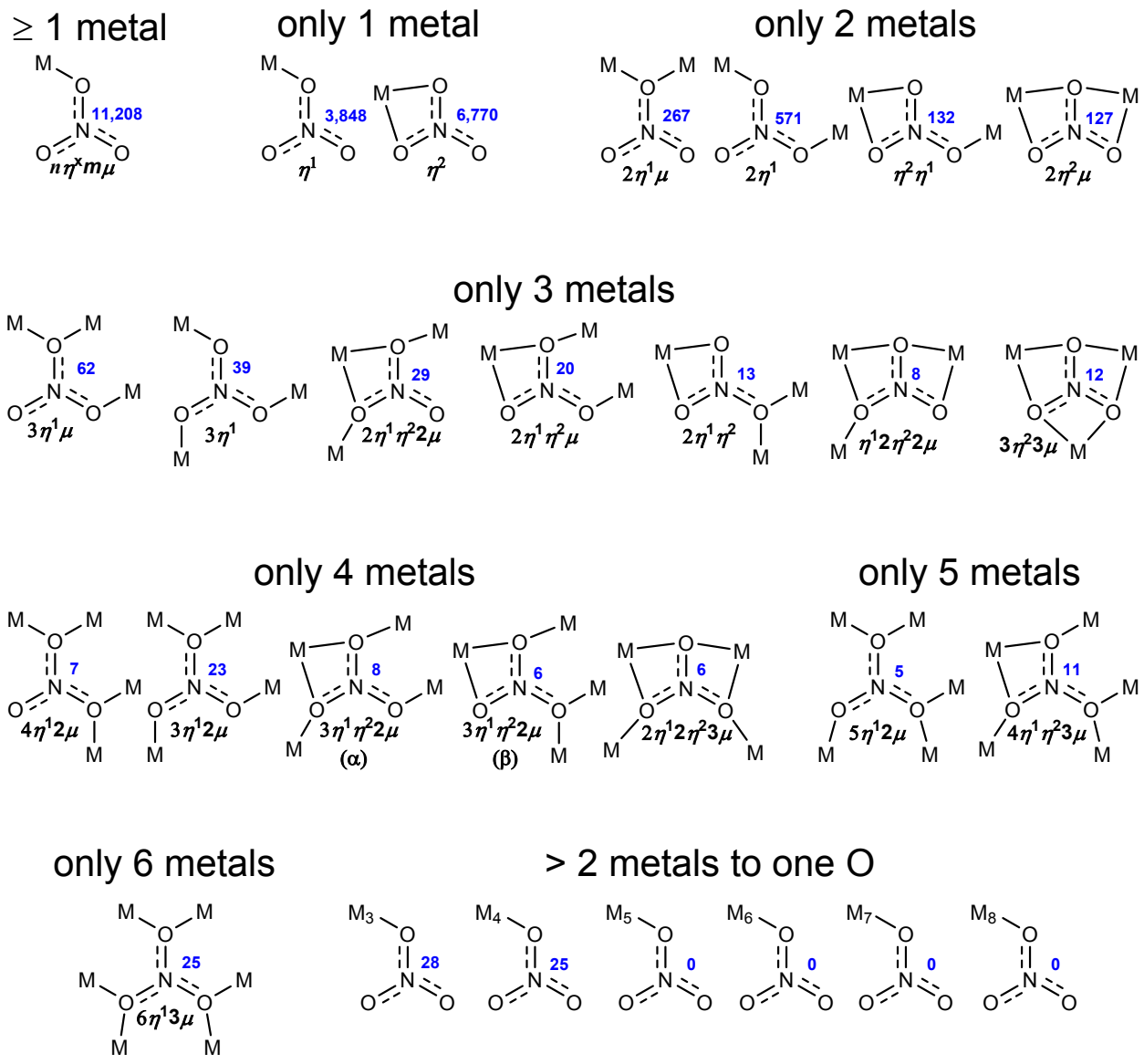

Figure S1. Overview of the different possible coordination modes found for an NO_3^- anion when coordinated to 1-6 metal atoms. The blue numbers represent the number of crystallographic information files (CIFs) found with that particular coordination mode. For the searches with at least one metal (top left) and for more than 2 metals coordinated to the same O-atom (bottom right) no restrictions were applied. For all other queries the number of attached atoms to the atoms belonging to NO_3^- were restricted to the number shown in the figure. For example, for η^1 the number of atoms bound to the coordinating O were set to two, and the others were set to one.

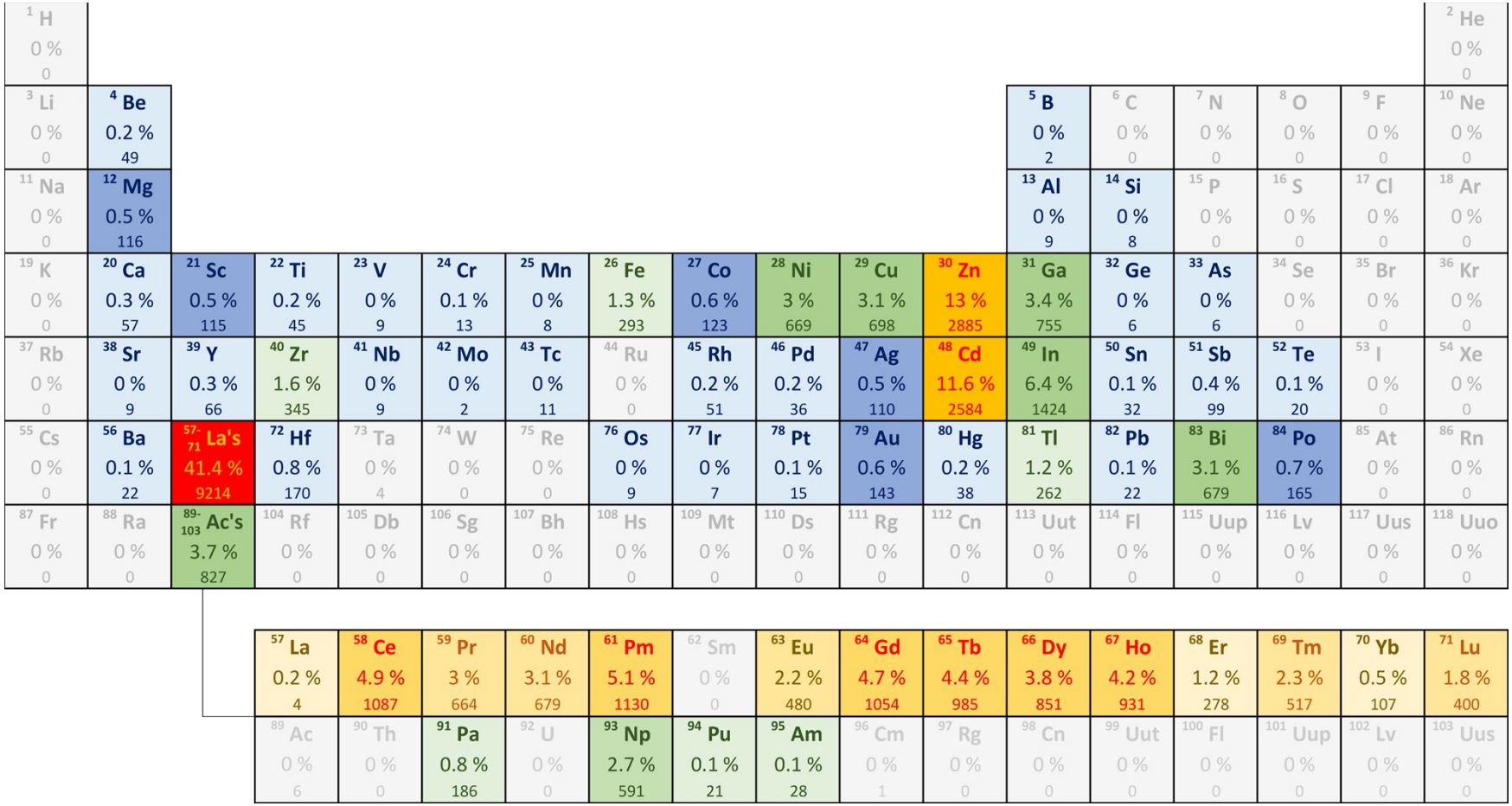

Figure S2. Schematic representation of the distribution of metals coordinated by a nitrate anion in any fashion. The data represents 22,241 NO_3– M structures found within 10,343 CIFs (NB: this deviates from the data in Figure S1 because the identity of M is not always given). The color code is meant as a guide to the eye, where red is the highest percentage of data and light blue the lowest.

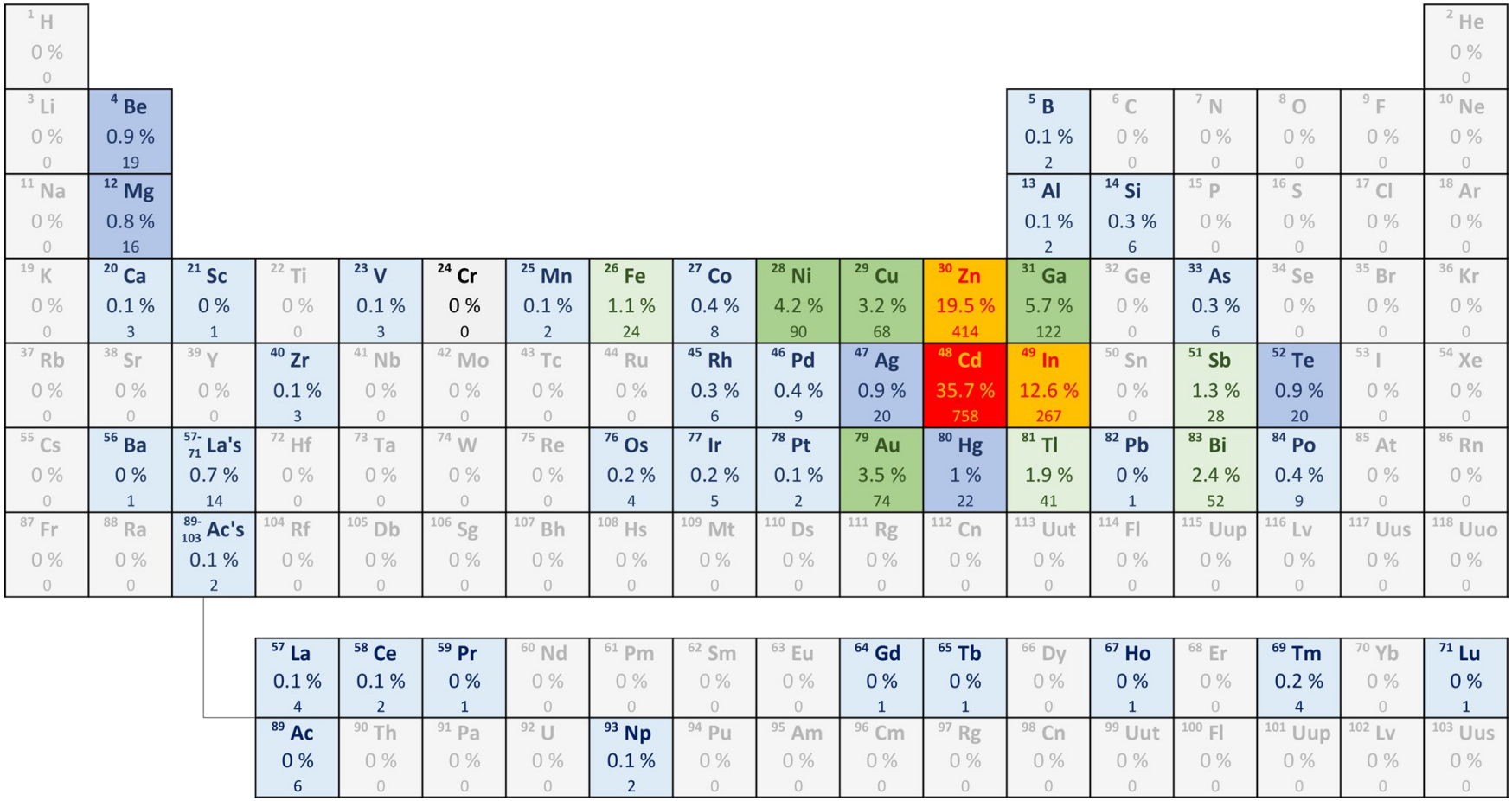

Figure S3. Schematic representation of the distribution of metals coordinated by a nitrate anion in a η^1 fashion (the M–O bond was specified as acyclic in conquest). The data represents 2,124 $O_2NO(\eta^1)$–M structures found within 1,403 CIFs (NB: this deviates from the data in Figure S1 because the identity of M is not always given). The color code is meant as a guide to the eye, where red is the highest percentage of data and light blue the lowest.

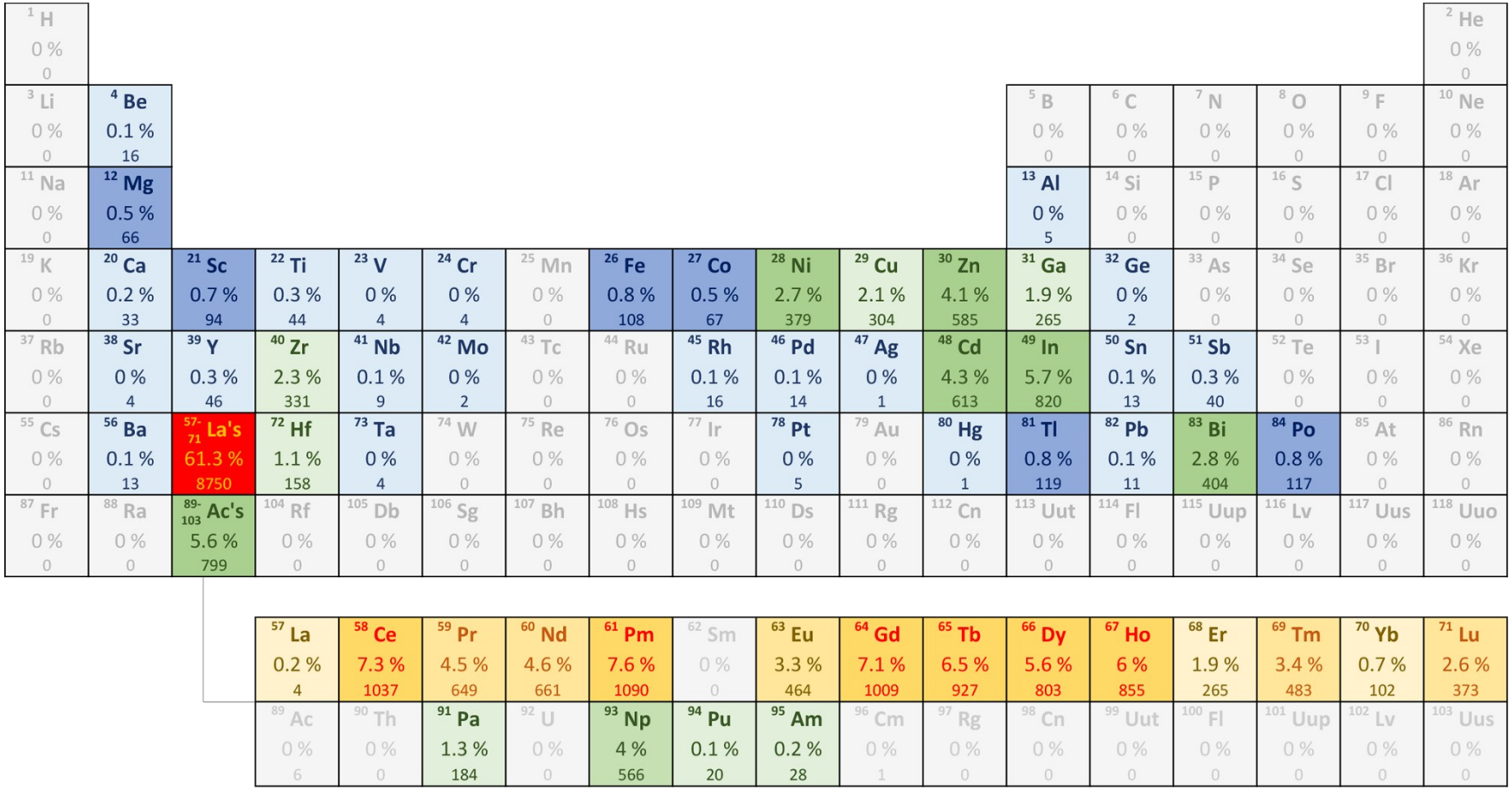

Figure S4. Schematic representation of the distribution of metals coordinated by a nitrate anion in a η^2 fashion. The data represents 14,266 $ONO_2(\eta^2)$–M structures found within 6,939 CIFs (NB: this deviates from the data in Figure S1 because the identity of M is not always given). The color code is meant as a guide to the eye, where red is the highest percentage of data and light blue the lowest.

Coord. mode[a]	Interact. partner[b]	CIFs	Hits	$r \leq 1$ Å	$n \leq \sum_{vdW}$ (%)[c]	Coord. mode[a]	Interact. partner[b]	CIFs	Hits	$r \leq 1$ Å	$n \leq \sum_{vdW}$ (%)[c]
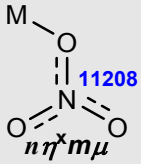	ElR^{Tx}	9,288	82,338	3,611	456 (12.6%)						
	N^{Tx}	7,621	32,200	1,328	32 (2.4%)						
	O^{Tx}	7,971	45,859	2,933	550 (18.8%)	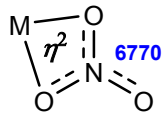	ElR^{Tx}	5,649	48,395	2,399	299 (12.5%)
	F^{Tx}	180	604	46	7 (15.2%)		$RO^{T2}H$	830	1,876	115	2 (1.7%)
	P^{Tx}	247	416	7	0		$R{=}O^{T1}$	3,443	9,493	874	217 (24.8%)
	S^{Tx}	665	1,730	69	0	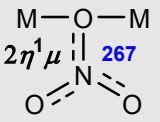	ElR^{Tx}	190	1,034	63	16 (25.4%)
	Cl^{Tx}	450	1,303	100	1 (1.0%)		$RO^{T2}H$	10	22	-	-
	As^{Tx}	5	6	0	0		$R{=}O^{T1}$	110	278	23	10 (38.5%)
	Se^{Tx}	13	27	1	0	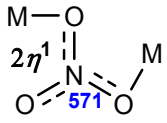	ElR^{Tx}	415	2,457	165	28 (17.0%)
	Br^{Tx}	72	155	12	0		$RO^{T2}H$	45	81	-	-
	I^{Tx}	14	38	2	0		$R{=}O^{T1}$	254	611	56	17 (30.4%)
	$R{=}O^{Tx}$	6,285	20,614	1,777	422 (23.7%)	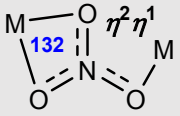	ElR^{Tx}	97	559	29	4 (13.8%)
	$R{=}O^{T1}$	5,902	18,029	1,680	406 (24.2%)		$RO^{T2}H$	9	12	-	-
	$RO^{Tx}H$	2,416	5,998	236	11 (4.7%)		$R{=}O^{T1}$	48	110	-	-
	$RO^{T2}H$	1,354	3,075	188	9 (4.8%)	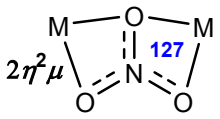	ElR^{Tx}	86	499	26	5 (19.0%)
	H_2O^{Tx}	1,418	3,443	105	7 (6.7%)		$RO^{T2}H$	6	13	-	-
	H_2O^{T2}	633	1,486	73	6 (8.2%)		$R{=}O^{T1}$	49	103	-	-
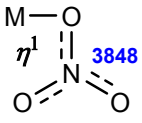	ElR^{Tx}	3,231	24,943	1,567	118 (11.6%)	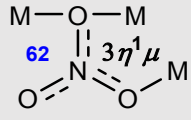	ElR^{Tx}	41	253	19	5 (26.3%)
	$RO^{T2}H$	471	870	40	2 (5%)		$RO^{T2}H$	1	2	-	-
	$R{=}O^{T1}$	2,136	6,319	596	126 (21.1%)		$R{=}O^{T1}$	27	80	-	-

Table S1. Numerical overview of searches performed for different coordination modes of a nitrate anions where an interacting partner has an intermolecular distance ≤ 5 Å from the NO_3^- N-atom. The entries highlighted in red are also shown in Table 1. [a]See also Figure S1 for structures; M = any metal and the number in blue indicates the number of CIFs found for that coordination mode. [b]The interacting partner considered in the search where R can be any atom and ElR can be N, P, As, O, S, Se, Te, F, Cl, Br, I, or At. The superscripts 'T1/T2/Tx' indicate the number of bonded atoms set in the ConQuest search where x means this was left unspecified. [c]The number of hits (also expressed as percentage) found within $r \leq 1$ Å where the interacting atom and the nitrate's N-atom are within each other's van der Waals radii.

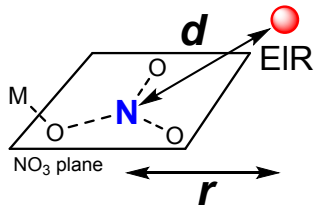

Figure S5. Simplified schematic of the most general query used, which contains all of the data in Table S1. The intermolecular N···EIR distance (***d***) was always set to ≤ 5 Å and the parallel displacement parameter (***r***, i.e. the radial displacement from N, parallel to the NO_3 plane) was derived from ***d*** and several other measurements. M = any metal, EIR = N, P, As, O, S, Se, Te, F, Cl, Br, I, or At. The bonds shown as dashed lines were set as any type of bond.

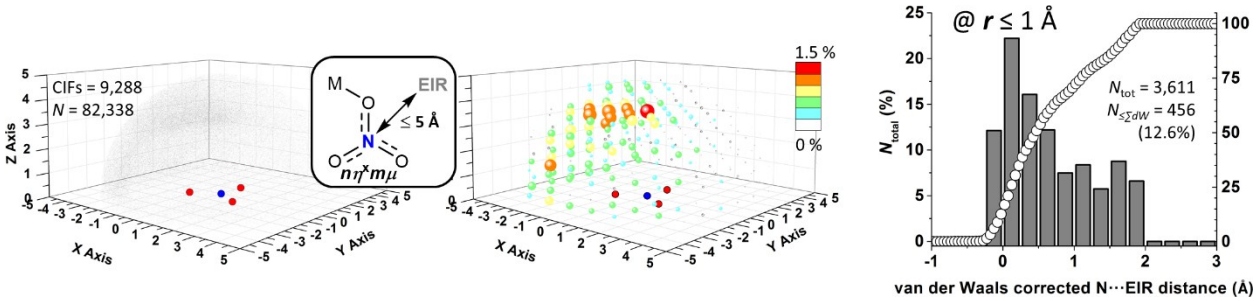

Figure S6. Three dimensional scatter plot (left) and four dimensional density plot (middle) for the most general dataset of $n\eta^x m\mu$ nitrate^N···EIR (see also inset figure). The data characterized by a parallel displacement parameter (***r***) of ≤ 1 Å was plotted as a function of the van der Waals corrected N···EIR distance (right) in both absolute (grey bars with left-hand scale) and cumulative percentages (open circles with right-hand scale).

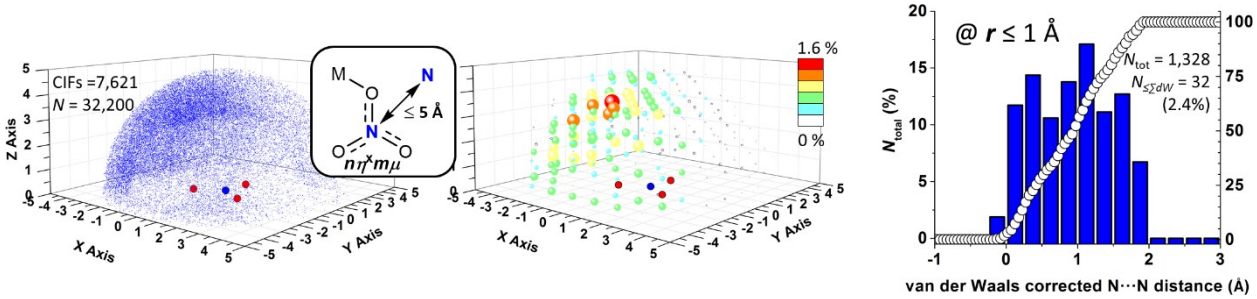

Figure S7. Three dimensional scatter plot (left) and four dimensional density plot (middle) for the dataset of $n\eta^x m\mu$ nitrate^N···N (see also inset figure). The data characterized by a parallel displacement parameter (***r***) of ≤ 1 Å was plotted as a function of the van der Waals corrected N···N distance (right) in both absolute (blue bars with left-hand scale) and cumulative percentages (open circles with right-hand scale).

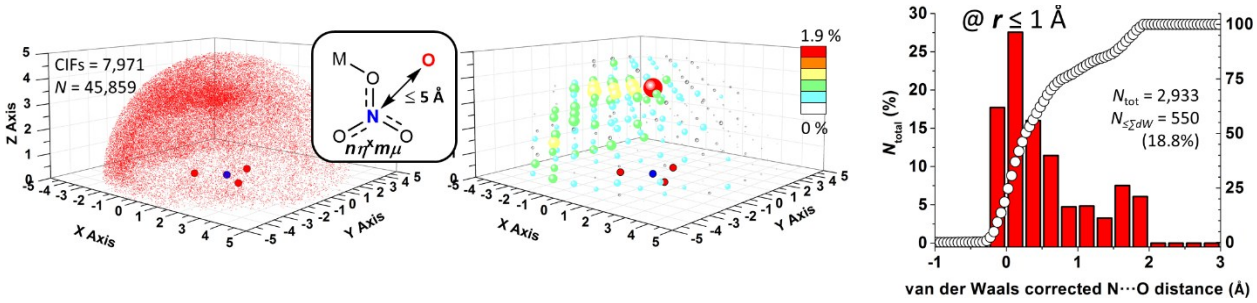

Figure S8. Three dimensional scatter plot (left) and four dimensional density plot (middle) for the dataset of $n\eta^x m\mu$ nitrate^N···O (see also inset figure). The data characterized by a parallel displacement parameter (***r***) of ≤ 1 Å was plotted as a function of the van der Waals corrected N···O distance (right) in both absolute (red bars with left-hand scale) and cumulative percentages (open circles with right-hand scale).

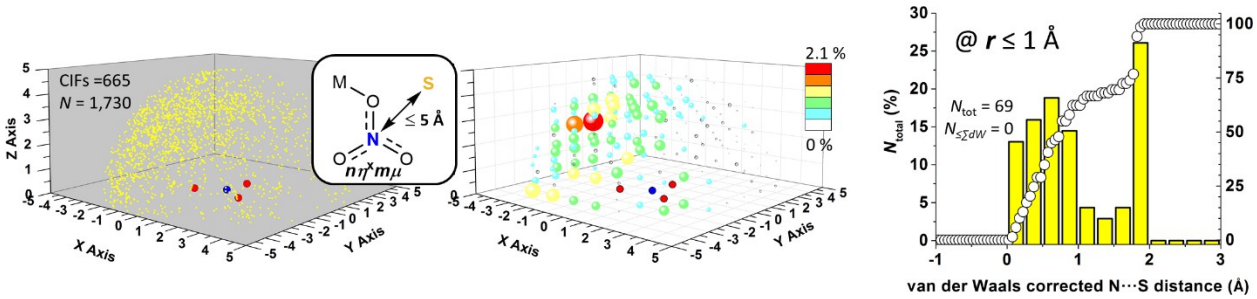

Figure S9. Three dimensional scatter plot (left) and four dimensional density plot (middle) for the dataset of $n\eta^x m\mu$ nitrate^N···S (see also inset figure). The data characterized by a parallel displacement parameter (***r***) of ≤ 1 Å was plotted as a function of the van der Waals corrected N···S distance (right) in both absolute (yellow bars with left-hand scale) and cumulative percentages (open circles with right-hand scale).

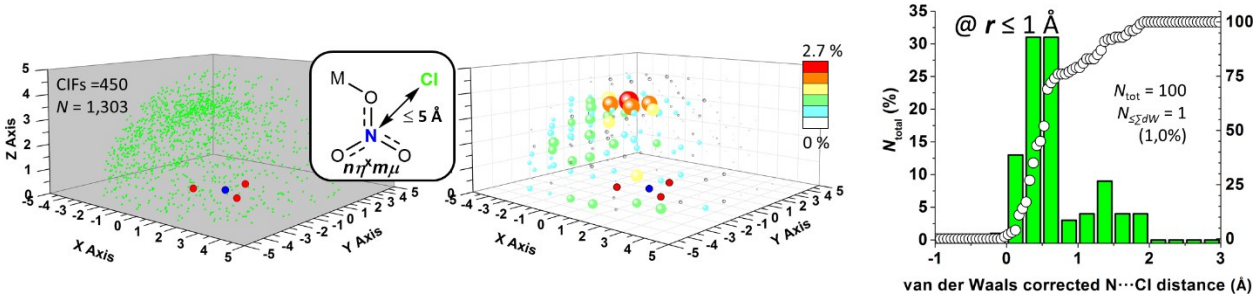

Figure S10. Three dimensional scatter plot (left) and four dimensional density plot (middle) for the dataset of $n\eta^x m\mu$ nitrate^N···Cl (see also inset figure). The data characterized by a parallel displacement parameter (***r***) of ≤ 1 Å was plotted as a function of the van der Waals corrected N···Cl distance (right) in both absolute (green bars with left-hand scale) and cumulative percentages (open circles with right-hand scale).

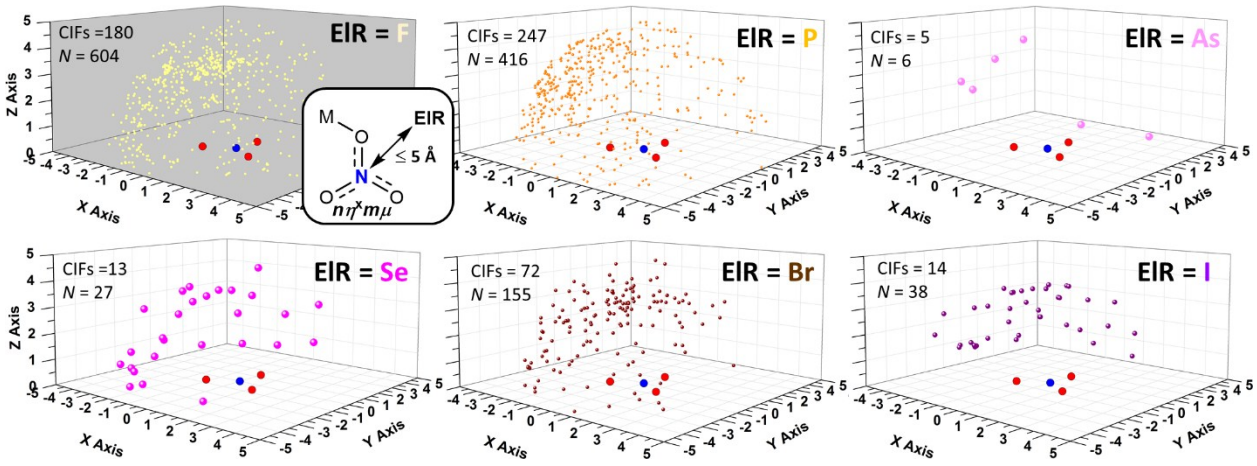

Figure S11. Three dimensional scatter plots for various $n\eta^x m\mu$ nitrate^N···ElR (see also inset figure) where ElR = F, P, As, Se, Br or I. Other plots (i.e. 4D/N(***r***)) were not generated because there were not enough hits (maximum of 604 for ElR = F). The number of data involved in van der Waals overlap at $\boldsymbol{r} \leq 1$ Å is given in Table S1.

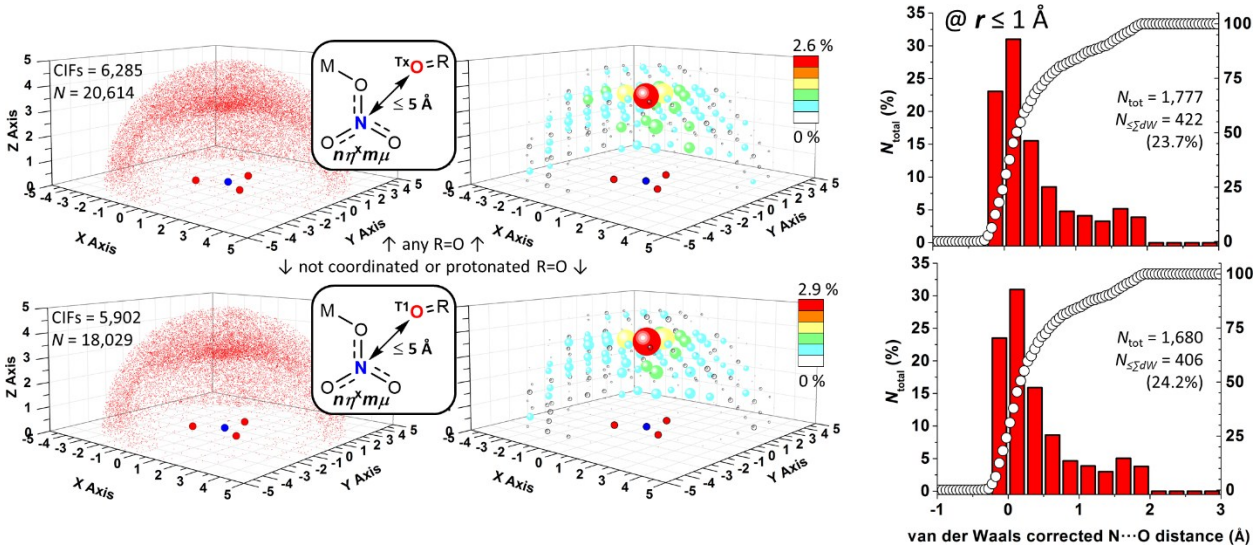

Figure S12. Three dimensional scatter plots (left) and four dimensional density plots (middle) for the datasets of $n\eta^x m\mu$ nitrate^N···O=R (see also inset figure, R = any atom). The data characterized by a parallel displacement parameter (***r***) of ≤ 1 Å was plotted as a function of the van der Waals corrected N···O distance (right) in both absolute (red bars with left-hand scale) and cumulative percentages (open circles with right-hand scale). The plots on the top represent any type of interacting R=O Oxygen atoms (indicated by 'Tx'), while the bottom plots concern only uncoordinated / unprotonated such O-atoms (indicated by 'T1').

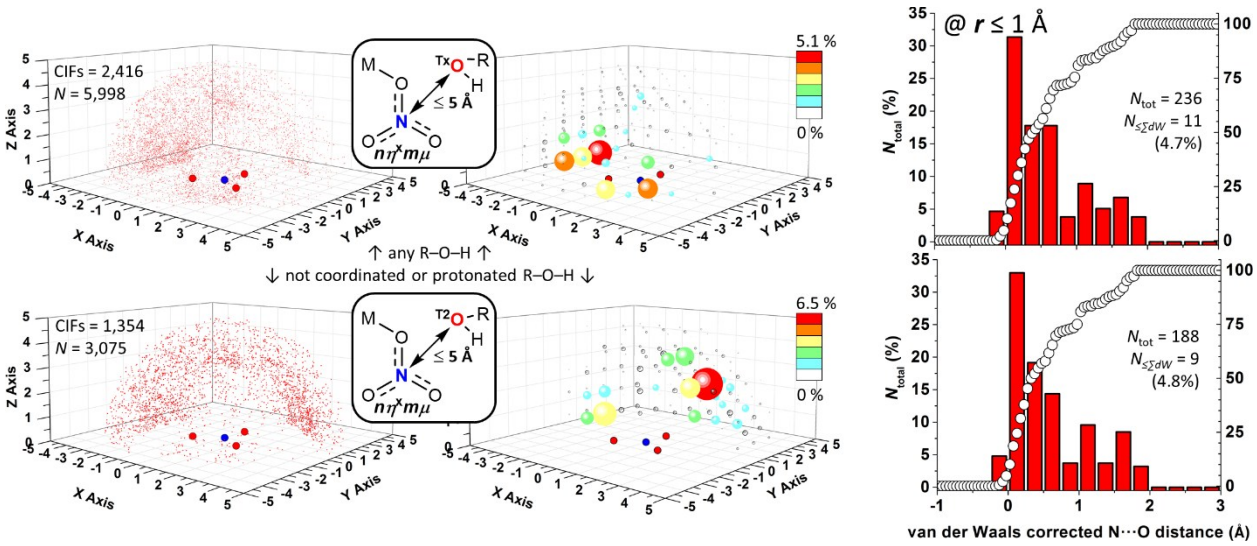

Figure S13. Three dimensional scatter plots (left) and four dimensional density plots (middle) for the datasets of $n\eta^x m\mu$ nitrate^N···OHR (see also inset figure, R = any atom). The data characterized by a parallel displacement parameter (***r***) of ≤ 1 Å was plotted as a function of the van der Waals corrected N···O distance (right) in both absolute (red bars with left-hand scale) and cumulative percentages (open circles with right-hand scale). The plots on the top represent any type of interacting ROH Oxygen atoms (indicated by 'Tx'), while the bottom plots concern only uncoordinated / unprotonated such O-atoms (indicated by 'T2').

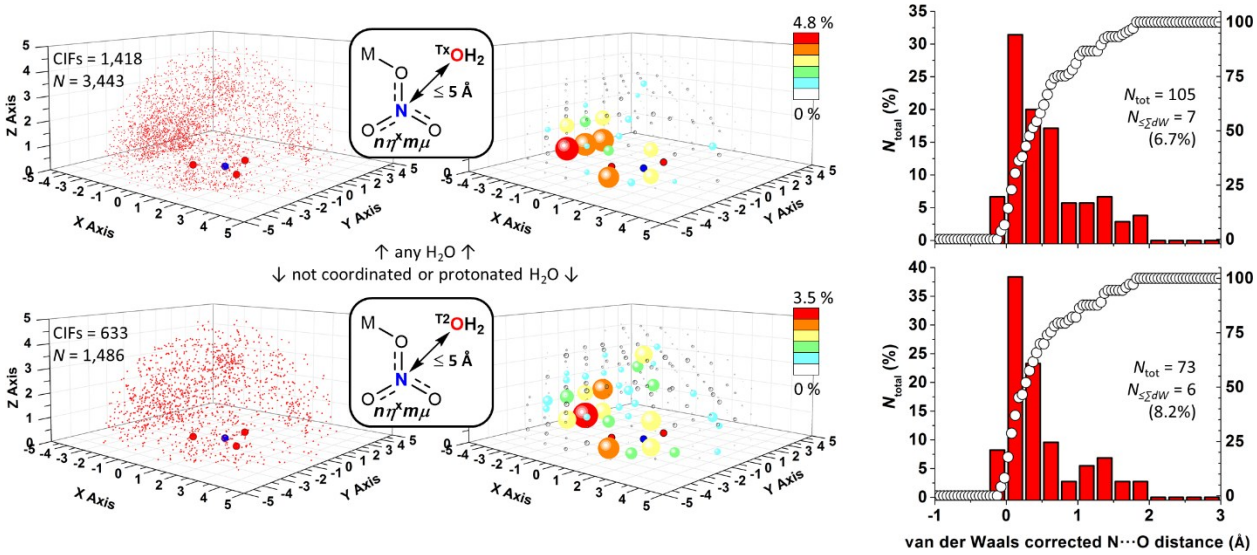

Figure S14. Three dimensional scatter plots (left) and four dimensional density plots (middle) for the datasets of $n\eta^x m\mu$ nitrate^N···OH_2 (see also inset figure, R = any atom). The data characterized by a parallel displacement parameter (***r***) of ≤ 1 Å was plotted as a function of the van der Waals corrected N···O distance (right) in both absolute (red bars with left-hand scale) and cumulative percentages (open circles with right-hand scale). The plots on the top represent any type of interacting OH_2 Oxygen atoms (indicated by 'Tx'), while the bottom plots concern only uncoordinated / unprotonated such O-atoms (indicated by 'T2').

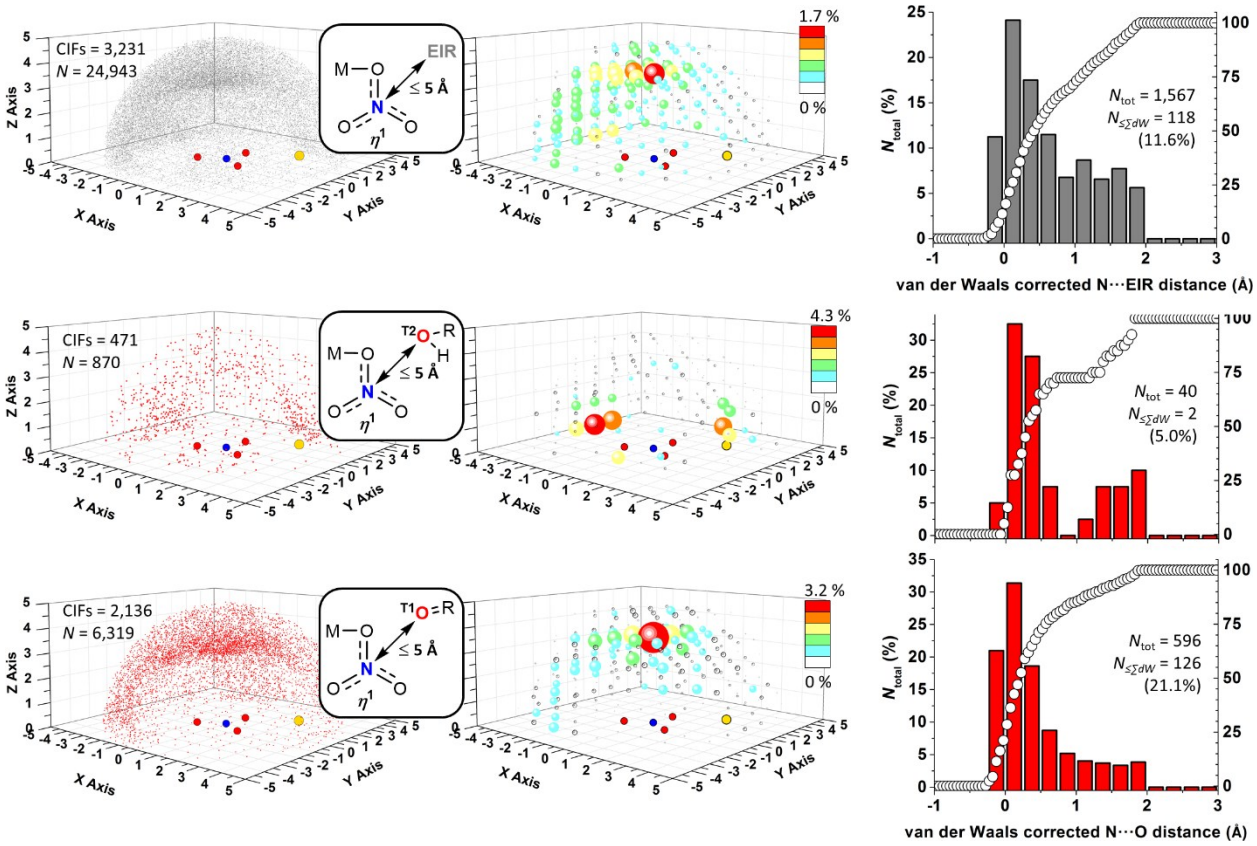

Figure S15. Three dimensional scatter plots (left) and four dimensional density plots (middle) for the datasets of η^1 nitrate^{N}···EIR (top) / ···ORH (middle) / ···O=R (bottom); see also inset figures (R = any atom, EIR = N, P, As, O, S, Se, Te, F, Cl, Br, I or At). The data characterized by a parallel displacement parameter (***r***) of ≤ 1 Å was plotted as a function of the van der Waals corrected N···EIR/O distance (right) in both absolute (bars with left-hand scale) and cumulative percentages (open circles with right-hand scale). The plots concerning 'EIR' represent any type of interacting electron rich atom, while the bottom plots with ORH and O=R concern only uncoordinated / unprotonated such O-atoms (indicated by 'T1/T2').

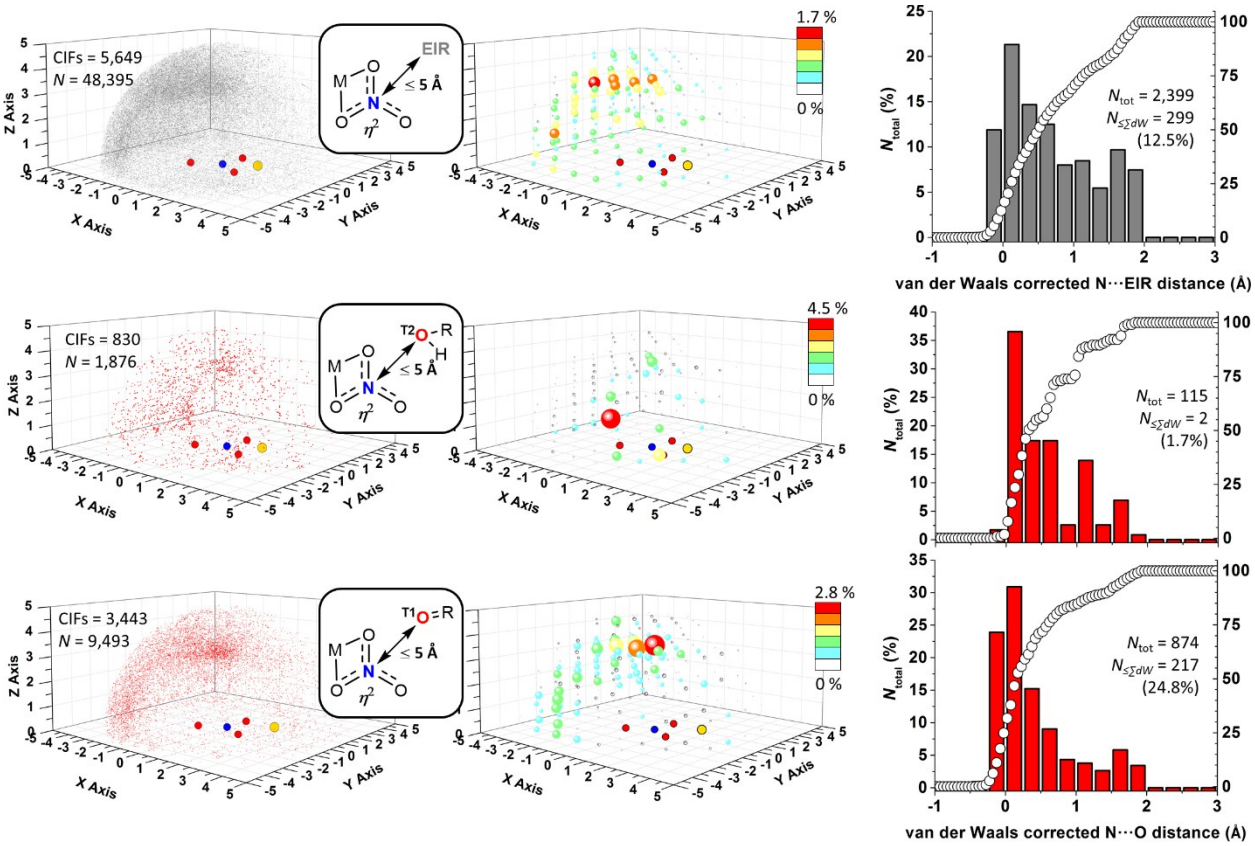

Figure S16. Three dimensional scatter plots (left) and four dimensional density plots (middle) for the datasets of η^2 nitrate^{N}···EIR (top) / ···ORH (middle) / ···O=R (bottom); see also inset figures (R = any atom, EIR = N, P, As, O, S, Se, Te, F, Cl, Br, I or At). The data characterized by a parallel displacement parameter (***r***) of ≤ 1 Å was plotted as a function of the van der Waals corrected N···EIR/O distance (right) in both absolute (bars with left-hand scale) and cumulative percentages (open circles with right-hand scale). The plots concerning 'EIR' represent any type of interacting electron rich atom, while the bottom plots with ORH and O=R concern only uncoordinated / unprotonated such O-atoms (indicated by 'T1/T2').

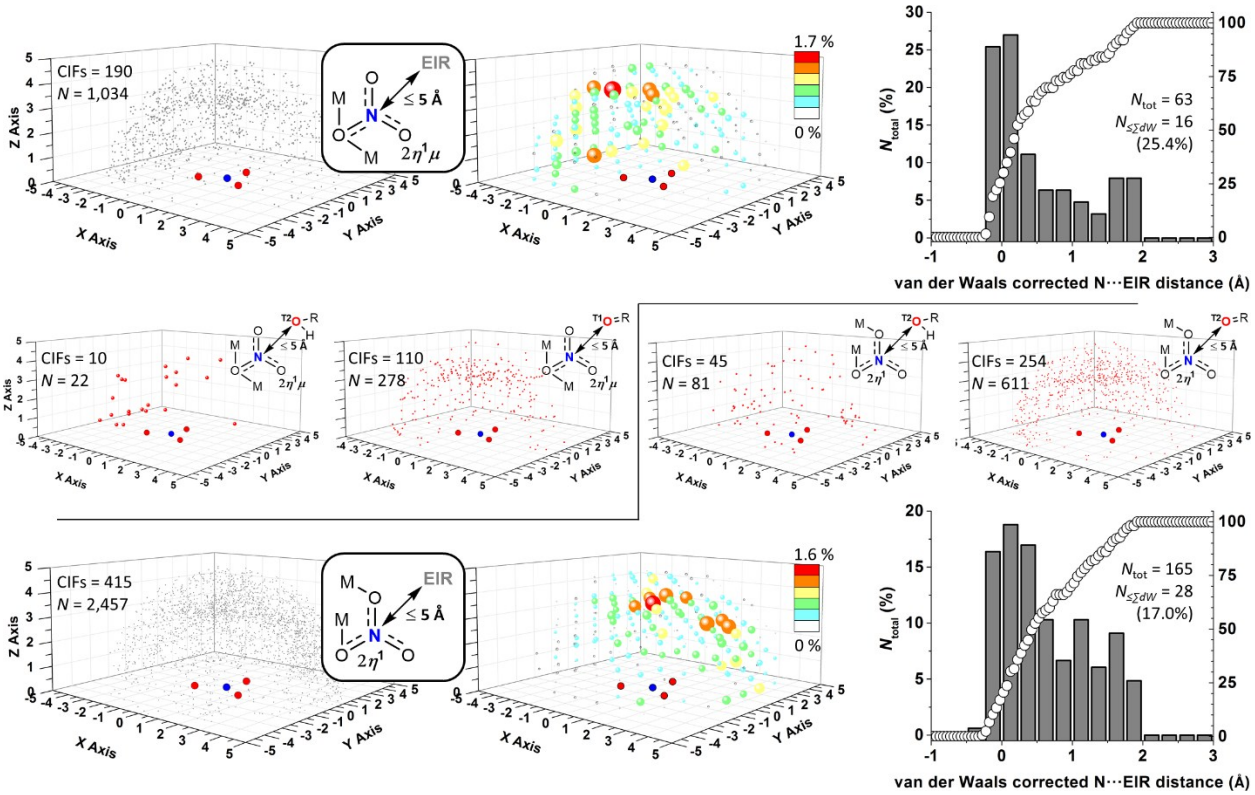

Figure S17. Three dimensional scatter plot (top left) and four dimensional density plot (top middle) for the dataset with $2\eta^1\mu$ nitrate^{N}···ElR (see also inset figure). Data characterized by a parallel displacement parameter (***r***) of ≤ 1 Å was plotted as a function of the van der Waals corrected N···ElR distance (top right) in both absolute (grey bars with left-hand scale) and cumulative percentages (open circles with right-hand scale). The three dimensional scatter plots are also given for $2\eta^1\mu$ nitrate^{N}···OHR and $2\eta^1\mu$ nitrate^{N} (center left, see also inset figures). The same plots are given for the dataset with $2\eta^1$ nitrate^{N} in the bottom (3D/4D/*N*(***r***) plots for ElR) and center right of the figure (3D plots for OHR and O=R). The plots concerning 'ElR' represent any type of interacting electron rich atom, while the plots with OHR and O=R concern only uncoordinated / unprotonated such O-atoms (indicated by 'T1/T2'). R = any atom and ElR = N, P, As, O, S, Se, Te, F, Cl, Br, I or At.

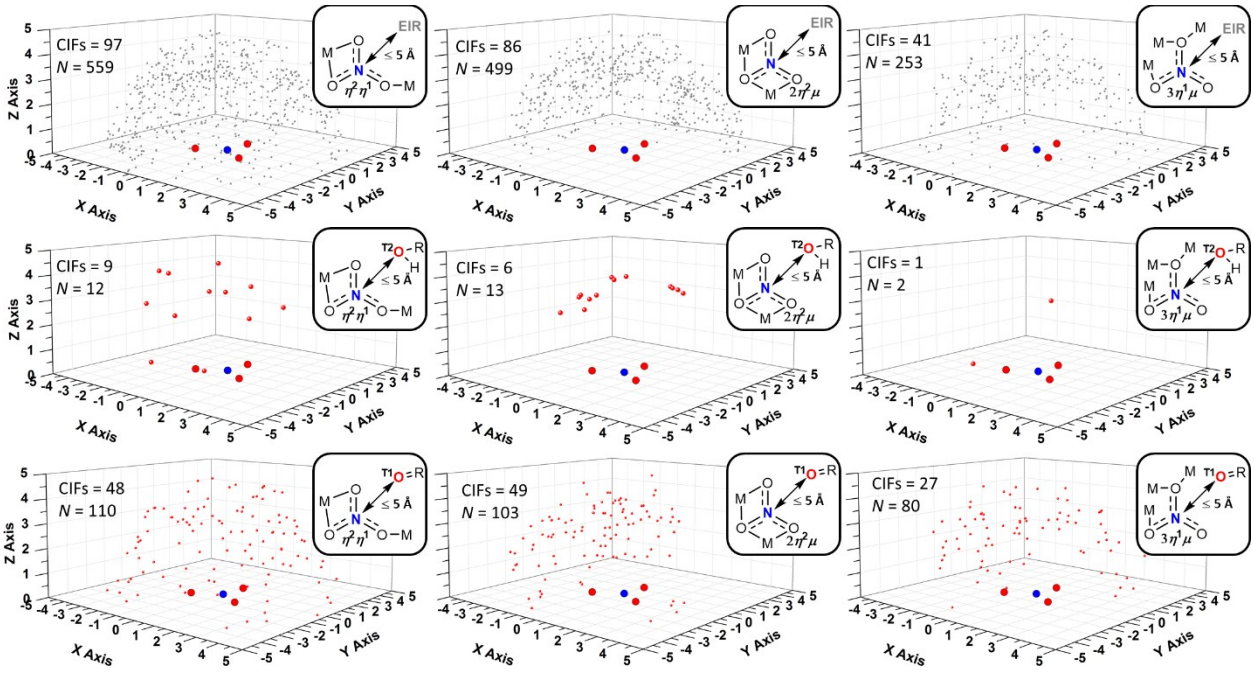

Figure S18. Three dimensional scatter plots of $\eta^2\eta^1$ (left), $2\eta^2\mu$ (middle) and $3\eta^1\mu$ (right) nitrate surrounded by ElR (top) OHR (middle) or O=R (bottom) moieties. Other plots (i.e. 4D/*N*(***r***)) were not generated because there were not enough hits (maximum of 559 for $\eta^2\eta^1$ nitrate$^{N}\cdots$ElR). The number of data involved in van der Waals overlap at $\boldsymbol{r} \leq 1$ Å for each nitrate coordination mode with any electron rich atoms is given in Table S1. The plots concerning 'ElR' represent any type of interacting electron rich atom, while the plots with OHR and O=R concern only uncoordinated / unprotonated such O-atoms (indicated by 'T1/T2'). R = any atom and ElR = N, P, As, O, S, Se, Te, F, Cl, Br, I or At.

Table S2. Overview of the 406 close contacts found within the CSD wherein an sp^2-hybridized O-atom is in close proximity to any coordinated nitrate anion's N-atom with a van der Waals corrected O···N distance (vdW) below 0 Å and a parallel displacement parameter (***r***) below 1 Å.

vdW	*r*	Refcode	sp^2-O	vdW	*r*	Refcode	sp^2-O	vdW	*r*	Refcode	sp^2-O
-0.022	0.431	KIJYIM01	Ag=O	-0.165	0.578	QAWSEO	NO_3	-0.069	0.690	GEZXOA	NO_3
-0.143	0.268	COJHAK10	Np=O	-0.164	0.116	UHECAL	NO_3	-0.068	0.139	BACNUQ	NO_3
-0.093	0.940	BAXQOI	U=O	-0.164	0.698	ADCDNO10	NO_3	-0.068	0.647	RIDTAZ	NO_3
-0.227	0.139	BOFVAV	U=O	-0.163	0.349	RIQQOZ	NO_3	-0.067	0.536	OPASEF	NO_3
-0.208	0.716	BOTYIS	U=O	-0.163	0.603	ETULIP	NO_3	-0.066	0.269	NUNYUR	NO_3
-0.134	0.562	BOTYIS	U=O	-0.162	0.467	GOFYIJ	NO_3	-0.066	0.435	WIJVES	NO_3
-0.152	0.280	COJGUD10	U=O	-0.156	0.817	PUBWIT	NO_3	-0.066	0.450	OFEWIH	NO_3
-0.130	0.483	DACCUI	U=O	-0.154	0.397	QOZWOR	NO_3	-0.066	0.672	HAVLUN	NO_3
-0.074	0.554	DACCUI	U=O	-0.150	0.361	NEXQIR	NO_3	-0.066	0.703	IDILUE	NO_3
-0.086	0.347	DACDAP	U=O	-0.150	0.697	FEZLIF	NO_3	-0.066	0.731	BURSOY	NO_3
-0.134	0.319	DEBRUZ	U=O	-0.150	0.932	LAMCIM	NO_3	-0.064	0.650	IWURAU	NO_3
-0.132	0.761	FAGNIL	U=O	-0.148	0.354	JAJYAV	NO_3	-0.064	0.929	LECWAS	NO_3
-0.091	0.867	FAGNIL	U=O	-0.148	0.492	LAVSOR01	NO_3	-0.063	0.702	HAVMEY	NO_3
-0.208	0.289	FISHIY	U=O	-0.148	0.577	BORNAG	NO_3	-0.062	0.124	JOLLEB	NO_3
-0.173	0.141	FISHIY	U=O	-0.147	0.470	IWUVIF	NO_3	-0.062	0.345	TIMJAA01	NO_3
-0.223	0.112	GIMSEC	U=O	-0.146	0.610	YUCXAW	NO_3	-0.062	0.359	OFEWIH	NO_3
-0.167	0.205	GOXGUX	U=O	-0.145	0.349	CIJRAQ	NO_3	-0.061	0.459	OFEWIH01	NO_3
-0.125	0.239	GOXGUX	U=O	-0.144	0.433	PIRDOL	NO_3	-0.061	0.522	QOGRAG	NO_3
-0.049	0.346	IPIJEX	U=O	-0.143	0.636	UQEMAF	NO_3	-0.060	0.288	MEHHIS	NO_3
-0.146	0.675	IXULIW	U=O	-0.143	0.987	EKAZOG	NO_3	-0.059	0.475	QOZSUT	NO_3
-0.034	0.963	IXULIW	U=O	-0.141	0.282	WIJVOC	NO_3	-0.059	0.854	CIZGAV	NO_3
-0.201	0.582	IXULOC	U=O	-0.137	0.257	LAVSOR01	NO_3	-0.059	0.955	VOSPIE	NO_3
-0.167	0.756	IXULOC	U=O	-0.137	0.457	VIZYIM	NO_3	-0.058	0.371	OFEWIH01	NO_3
-0.091	0.558	IXULOC	U=O	-0.136	0.190	CANCEZ	NO_3	-0.058	0.573	YATVIA	NO_3
-0.087	0.485	LAJYIH	U=O	-0.136	0.360	AFIWOC	NO_3	-0.058	0.674	GEZXUG	NO_3
-0.065	0.841	LURBAC	U=O	-0.136	0.525	MABQOX	NO_3	-0.058	0.746	XAYTUN	NO_3
-0.078	0.048	MIDXAY	U=O	-0.135	0.310	OLUZUS	NO_3	-0.058	0.964	LAVSOR	NO_3
-0.170	0.691	PIDJAP	U=O	-0.135	0.448	ITOMEL	NO_3	-0.057	0.434	AXUYEY	NO_3
-0.152	0.418	PIDJAP	U=O	-0.135	0.470	LECWOG	NO_3	-0.057	0.659	QAVVOY	NO_3
-0.152	0.789	RUGGAC	U=O	-0.135	0.481	CAQFUV	NO_3	-0.057	0.907	QEPLAA	NO_3
-0.175	0.322	RUWBER	U=O	-0.135	0.513	LECYAU	NO_3	-0.056	0.255	QAQNON	NO_3
-0.237	0.389	RUWBIV	U=O	-0.135	0.556	IWUROI	NO_3	-0.056	0.381	ELIQUM	NO_3
-0.148	0.264	SENMUT	U=O	-0.134	0.086	FUWDOS	NO_3	-0.055	0.496	OHIXIO	NO_3
-0.020	0.101	SENMUT	U=O	-0.134	0.351	AZEXIM	NO_3	-0.055	0.504	XEQYID	NO_3
-0.281	0.258	UYENIW	U=O	-0.133	0.807	EGUMEA01	NO_3	-0.055	0.904	BOPJUM	NO_3
-0.052	0.633	VOSPUQ	U=O	-0.132	0.438	FAWKUJ	NO_3	-0.054	0.216	TUMHAM	NO_3
-0.211	0.132	WIJVES	U=O	-0.132	0.759	QOYDIR	NO_3	-0.054	0.795	KUPLUD	NO_3
-0.197	0.425	WIJVES	U=O	-0.132	0.993	CINXOM	NO_3	-0.054	0.874	QEPLEE	NO_3

-0.144	0.395	WIJVES	U=O	-0.131	0.981	VIZYIM	NO_3	-0.054	0.961	HERWAC	NO_3
-0.117	0.937	XEPXUM	U=O	-0.130	0.450	ATOCIV01	NO_3	-0.053	0.174	WUNFAM02	NO_3
-0.079	0.566	XEPXUM	U=O	-0.129	0.086	SEFNIB	NO_3	-0.053	0.260	WIYHIV	NO_3
-0.087	0.493	XUGJIU	U=O	-0.129	0.326	AXIREE	NO_3	-0.053	0.349	TIMJAA	NO_3
-0.220	0.117	UTIPAQ	C=O	-0.129	0.734	UXIHEQ	NO_3	-0.052	0.604	AFEGEY01	NO_3
-0.198	0.179	TEPNOT	C=O	-0.128	0.345	ZOQGOB	NO_3	-0.051	0.054	LABWEQ	NO_3
-0.179	0.227	TEPNUZ	C=O	-0.128	0.402	WADMOE	NO_3	-0.050	0.226	BACPAY	NO_3
-0.161	0.207	TEPPAH	C=O	-0.128	0.786	EGUMEA02	NO_3	-0.050	0.269	KIPYIT	NO_3
-0.144	0.422	SIDVIL	C=O	-0.128	0.905	LAMCOS	NO_3	-0.048	0.675	HAYZOY	NO_3
-0.110	0.216	GEBKUT	C=O	-0.127	0.075	VUKWIJ	NO_3	-0.046	0.227	NAFDUU01	NO_3
-0.076	0.765	EJEWUM	C=O	-0.127	0.619	TOKZOI	NO_3	-0.045	0.632	FELYAW	NO_3
-0.075	0.460	FINLEV	C=O	-0.127	0.636	RUMPIY	NO_3	-0.045	0.817	FOCREU	NO_3
-0.041	0.167	FIVHAV	C=O	-0.126	0.813	NUYMEA	NO_3	-0.044	0.496	QOZWUX	NO_3
-0.041	0.917	UYAQUI	C=O	-0.126	0.907	LAMCEI	NO_3	-0.043	0.179	XEPXUM	NO_3
-0.147	0.395	IPASOH	C=O	-0.125	0.807	EGUMEA03	NO_3	-0.042	0.669	HAVLEX	NO_3
-0.113	0.627	YUVPOV	**C=O**[a]	-0.124	0.200	TIGGUN	NO_3	-0.041	0.564	JIQYOY	NO_3
-0.298	0.715	NUSKAO	R-NO_2	-0.124	0.273	ATOHUM	NO_3	-0.041	0.590	YEBNAV	NO_3
-0.211	0.756	PITHEH	R-NO_2	-0.124	0.967	LEWDIC	NO_3	-0.040	0.374	VOWKEZ	NO_3
-0.188	0.490	NUSJUH	R-NO_2	-0.124	0.997	XUGJIU	NO_3	-0.040	0.651	UQEYEW	NO_3
-0.178	0.502	OQIKIJ	R-NO_2	-0.121	0.337	QOCYAI	NO_3	-0.040	0.685	LACDEY	NO_3
-0.118	0.618	WECVUX	R-NO_2	-0.120	0.611	WAKNIH	NO_3	-0.040	0.846	GOCLOA	NO_3
-0.275	0.426	YIKXEV	Cl=O	-0.120	0.983	YONPOI	NO_3	-0.039	0.675	EQUNIO	NO_3
-0.014	0.429	NEVHIH	Cl=O	-0.119	0.802	EGUMEA	NO_3	-0.039	0.905	CIZGEZ	NO_3
-0.106	0.592	YONPUO	**S=O**[b]	-0.118	0.955	TUZLAB	NO_3	-0.039	0.940	LAJXOK	NO_3
-0.202	0.111	XAFFAM01	Re-N=O	-0.117	0.063	WOZXIS	NO_3	-0.037	0.337	CAKSUD	NO_3
-0.016	0.513	YUWWAO	NO_3	-0.117	0.196	DAPCUN02	NO_3	-0.037	0.834	WEPKOR	NO_3
-0.068	0.242	UVITUQ	NO_3	-0.117	0.403	PITHEH	NO_3	-0.036	0.495	SUMGIR	NO_3
-0.226	0.453	WIJVES	NO_3	-0.117	0.502	PAZMOT	NO_3	-0.035	0.369	TANYIR	NO_3
-2.247	0.532	GUVJAK	NO_3	-0.117	0.687	YIYBEP	NO_3	-0.035	0.601	LUKQOY	NO_3
-0.385	0.968	SICCOX	NO_3	-0.117	0.803	CEPMAM01	NO_3	-0.035	0.646	UQEYEW	NO_3
-0.358	0.988	CUMYAM	NO_3	-0.117	0.925	FOGGUF	NO_3	-0.034	0.393	DIGLOV	NO_3
-0.307	0.187	FETYEK	NO_3	-0.116	0.277	GUKZOD	NO_3	-0.033	0.197	LAVSOR	NO_3
-0.306	0.448	TULHAK	NO_3	-0.116	0.968	SISQOB	NO_3	-0.033	0.655	IGURAE	NO_3
-0.291	0.362	IFOHER	NO_3	-0.115	0.449	XAFFAM01	NO_3	-0.033	0.839	CIZGUP	NO_3
-0.271	0.640	UCUGIJ	NO_3	-0.115	0.471	CIMVAX	NO_3	-0.032	0.668	EQUNOU	NO_3
-0.257	0.214	IWUVIF	NO_3	-0.114	0.594	IMZNCU03	NO_3	-0.031	0.164	BUXMUE	NO_3
-0.254	0.722	USEBAX	NO_3	-0.112	0.517	GAKWAQ	NO_3	-0.031	0.467	CECSAF	NO_3
-0.250	0.040	MUPHUB	NO_3	-0.112	0.812	BEYREE	NO_3	-0.030	0.056	ZAZXIJ	NO_3
-0.249	0.320	ATOHUM	NO_3	-0.112	0.994	FORCAR	NO_3	-0.030	0.237	CIYJIE	NO_3
-0.245	0.533	ALUNEA	NO_3	-0.109	0.337	YATVIA	NO_3	-0.030	0.310	CIJTIY	NO_3
-0.243	0.097	YEBQIG	NO_3	-0.109	0.376	WAKNAZ	NO_3	-0.028	0.408	EFIZUO	NO_3

-0.241	0.564	OZOXEH	NO_3	-0.109	0.516	IMZNCU03	NO_3	-0.028	0.636	RUYMIJ	NO_3
-0.238	0.932	EMUCIA	NO_3	-0.109	0.654	YUFWIH01	NO_3	-0.027	0.868	CIZGOJ	NO_3
-0.236	0.375	ALUNEA	NO_3	-0.109	0.672	EQUNUA	NO_3	-0.026	0.387	VETFAC	NO_3
-0.235	0.206	CEPMAM	NO_3	-0.107	0.626	TORGUE	NO_3	-0.026	0.621	JAFWOD	NO_3
-0.232	0.110	EYUCIL	NO_3	-0.107	0.807	QAWSEO	NO_3	-0.026	0.811	JAMDIK	NO_3
-0.228	0.317	COZRAM	NO_3	-0.106	0.643	CIHYUP	NO_3	-0.024	0.107	KUYWAE	NO_3
-0.226	0.226	GUVHUC	NO_3	-0.106	0.709	EVONUA	NO_3	-0.024	0.242	VIDYIQ	NO_3
-0.224	0.200	QEKJOG	NO_3	-0.106	0.868	ELIRAT	NO_3	-0.024	0.635	YIYROO	NO_3
-0.221	0.687	VUHFUA	NO_3	-0.105	0.479	PAXQEK	NO_3	-0.023	0.382	LONTAJ	NO_3
-0.220	0.322	IZOJOW	NO_3	-0.105	0.479	PAXQEK01	NO_3	-0.023	0.499	AXIHUK	NO_3
-0.220	0.717	CEPMAM	NO_3	-0.105	0.595	BADXEL	NO_3	-0.023	0.521	IMZNCU	NO_3
-0.219	0.287	YEWWUU	NO_3	-0.105	0.595	BADXEL01	NO_3	-0.023	0.555	XUKYIN	NO_3
-0.219	0.404	OFIZIN	NO_3	-0.104	0.438	KEZZEW	NO_3	-0.023	0.564	PIRZUM	NO_3
-0.218	0.340	PEBWIE	NO_3	-0.104	0.652	PAZMIN	NO_3	-0.023	0.677	IWURUO	NO_3
-0.218	0.483	IZOJIQ	NO_3	-0.104	0.735	ALABAS	NO_3	-0.023	0.853	XAYTIB	NO_3
-0.216	0.296	HIPPIG	NO_3	-0.103	0.481	YONQAV	NO_3	-0.022	0.571	WODSOY	NO_3
-0.213	0.508	WEFWIO	NO_3	-0.101	0.333	EHALII	NO_3	-0.021	0.614	QAWSOY	NO_3
-0.207	0.488	OPASEF	NO_3	-0.101	0.597	PAZMEJ	NO_3	-0.020	0.432	BIZTIN	NO_3
-0.206	0.156	IBAQIM	NO_3	-0.099	0.593	AGIFIH	NO_3	-0.020	0.445	KATFEQ	NO_3
-0.203	0.394	SIXVOL	NO_3	-0.097	0.463	WIJVOC	NO_3	-0.020	0.789	QOZWIL	NO_3
-0.201	0.223	AMBZPB10	NO_3	-0.094	0.357	FAWKOD	NO_3	-0.020	0.881	HECFOL	NO_3
-0.201	0.398	ATOCIV	NO_3	-0.094	0.533	TOJGAB	NO_3	-0.019	0.427	SOLKAF	NO_3
-0.200	0.491	NEXQIR	NO_3	-0.093	0.646	QEKKIB	NO_3	-0.019	0.450	QAQPEF	NO_3
-0.199	0.585	NEXQIR	NO_3	-0.091	0.229	ZAZXOP	NO_3	-0.017	0.194	UJAZAG	NO_3
-0.197	0.355	WUZNEM	NO_3	-0.089	0.480	ATOCIV02	NO_3	-0.017	0.390	LIYMIP	NO_3
-0.195	0.487	BUSSAL	NO_3	-0.089	0.614	ITOMOV	NO_3	-0.016	0.670	OBUBET	NO_3
-0.195	0.604	REWTES	NO_3	-0.087	0.500	XARWES	NO_3	-0.016	0.978	DOYXOF	NO_3
-0.195	0.642	TEBTEA	NO_3	-0.085	0.100	BACPAY	NO_3	-0.015	0.653	MALKAL	NO_3
-0.194	0.508	VIXPIB	NO_3	-0.084	0.994	FOGGIT	NO_3	-0.015	0.718	IWUSAV	NO_3
-0.193	0.288	TUZLAB	NO_3	-0.083	0.167	LAVSOR	NO_3	-0.015	0.781	MALKOZ	NO_3
-0.193	0.614	BORNAG01	NO_3	-0.083	0.784	QOCYAI	NO_3	-0.015	0.853	HOPZIW	NO_3
-0.188	0.280	NEXQIR	NO_3	-0.083	0.913	VOSPOK	NO_3	-0.014	0.258	QOZVOQ	NO_3
-0.186	0.322	ITEPIH	NO_3	-0.082	0.404	SABNIT01	NO_3	-0.014	0.579	XUCGAE	NO_3
-0.185	0.452	XIYYOT	NO_3	-0.082	0.405	XEQYID	NO_3	-0.014	0.741	PILYAK	NO_3
-0.184	0.399	BOFLIS	NO_3	-0.082	0.482	MOKKAA	NO_3	-0.012	0.307	IDUFIX	NO_3
-0.184	0.584	KIPYIT	NO_3	-0.080	0.437	WUYYUK	NO_3	-0.012	0.498	YILHIL	NO_3
-0.183	0.480	AFOGIM	NO_3	-0.080	0.632	ZUQWAL	NO_3	-0.012	0.602	IPASOH	NO_3
-0.183	0.577	KIGSUP	NO_3	-0.080	0.639	TIJCEU	NO_3	-0.011	0.161	PUZFOG	NO_3
-0.182	0.799	ATOCUJ	NO_3	-0.079	0.785	WAKNON	NO_3	-0.011	0.634	XIZQUS	NO_3
-0.181	0.361	JADMUZ	NO_3	-0.078	0.777	AQIVON	NO_3	-0.011	0.685	MABQOX	NO_3
-0.181	0.573	XOLMAM	NO_3	-0.077	0.639	PENZEO	NO_3	-0.011	0.752	OHIXEK	NO_3

-0.181	0.720	QOYDIR02	NO_3	-0.077	0.745	ASAFEF	NO_3	-0.011	0.762	GEPFIS	NO_3
-0.181	0.818	VEQNEM	NO_3	-0.076	0.099	KEBFAY01	NO_3	-0.010	0.166	EHALII	NO_3
-0.180	0.321	JAJYEZ	NO_3	-0.076	0.104	BACNUQ	NO_3	-0.010	0.803	LURFIO	NO_3
-0.180	0.618	EVOLAC	NO_3	-0.076	0.717	XEVQEW	NO_3	-0.009	0.643	AFEGEY	NO_3
-0.179	0.878	HELGUA	NO_3	-0.075	0.659	TASPEK	NO_3	-0.008	0.227	NCIMCU	NO_3
-0.178	0.237	YUYDAZ	NO_3	-0.072	0.307	HISSUY	NO_3	-0.008	0.310	QAQPAB	NO_3
-0.178	0.719	ELUKIF	NO_3	-0.072	0.322	NDPYAG	NO_3	-0.008	0.462	BAWDIM11	NO_3
-0.177	0.682	BORNAG02	NO_3	-0.072	0.475	YUYDAZ	NO_3	-0.008	0.526	MIYWOH	NO_3
-0.174	0.639	MIYWOH	NO_3	-0.072	0.782	EFIZUO	NO_3	-0.007	0.491	IBOFEL	NO_3
-0.172	0.488	TISKAJ	NO_3	-0.072	0.909	MOYRIB	NO_3	-0.006	0.633	HELGOU	NO_3
-0.172	0.562	QAWSOY	NO_3	-0.071	0.957	LAMCAE	NO_3	-0.006	0.663	ZICZAO	NO_3
-0.168	0.189	GIHLIU	NO_3	-0.070	0.045	MICVEA	NO_3	-0.006	0.690	RIXFOU	NO_3
-0.168	0.338	OMABAH	NO_3	-0.070	0.415	NOQTAP	NO_3	-0.005	0.576	YIYRII	NO_3
-0.168	0.567	PUBWEP	NO_3	-0.070	0.575	KEXHUQ	NO_3	-0.005	0.782	QOZWEH	NO_3
-0.165	0.050	DAYMOG	NO_3	-0.070	0.661	UYENIW	NO_3	-0.004	0.593	ETOXUH	NO_3
-0.165	0.340	IZOJOW	NO_3								

[a]The structure involves a co-crystallized acetone molecule. [b]The structure involves a co-crystallized dimethyl sulfoxide molecule.

References

1. F. H. Allen, *Acta Crystallogr. B*, 2002, **58**, 380-388.
2. A. Bauza, A. Frontera and T. J. Mooibroek, *Cryst. Growth Des.*, 2016, **16**, 5520-5524.
3. A. Bauza, A. Frontera and T. J. Mooibroek, *Nat. Commun.*, 2017, **8**, Art. Nr. 14522.
4. T. J. Mooibroek and P. Gamez, *CrystEngComm*, 2012, **14**, 8462-8467.